

Final Report for NASA – Grant NAG 8-1445

Studies of Atomic Free Radicals Stored in a Cryogenic Environment

David M. Lee, Principal Investigator
Laboratory of Atomic and Solid State Physics, Clark Hall 117
Cornell University, Ithaca, NY 14853-2501, USA
(Dated: April 30, 2003)

FAX (607) 255-6428
e-mail dml20@cornell.edu

Marshall Space Flight Center Technical Monitor
Dorothy Hubbard & Glen Alexander

INTRODUCTION.

This research program has been devoted to the study of impurity - helium solids which are shown to be composed of impurity atoms, molecules and clusters of atoms and molecules, each surrounded by a thin layer of inert solid helium mainly in the temperature range between 1 and 4 K. The impurity clusters cling together to form loosely structured porous solids. The pores are typically filled with liquid helium although it is possible to prepare free standing dry solids by draining out the liquid helium. Information obtained in this research program from structural studies employing ultrasound and x ray scattering techniques have verified this picture. Impurity solids form an excellent medium for the storage of atomic free radicals. The thin layers of inert solid helium retard the recombination of these atoms into molecules by restricting diffusion. These materials therefore provide the possibility of storing large quantities of chemical energy. Impurities incorporated in these gel-like solids range from heavy atoms (krypton, neon) and molecules (nitrogen) to the very lightest impurities including H₂, D₂, HD molecules and hydrogen and deuterium atoms. For the lightest atoms, quantum overlap will occur at very low temperatures (< 0.1K) for the average concentrations presently achieved in our work, ($10^{17} - 10^{18}$ atoms/cm³). The condition required is that the thermal de Broglie wave length must become comparable to the mean separation between atoms. If the quantum overlap condition is satisfied and the mobility of the atoms is sufficient, a quantum fluid consisting of hydrogen atoms or deuterium atoms can be achieved. By observing the time for hydrogen atoms to recombine to form H₂ molecules, we have found that hydrogen atoms are considerably more mobile than deuterium atoms in impurity-helium solids and therefore may be a better candidate for exhibiting quantum fluid behavior. The most fascinating possibility would be for a quantum fluid of hydrogen impurity atoms to undergo Bose-Einstein condensation, which is a subject of great current interest. The most important tool in our laboratory for the study of atom concentrations is the electron paramagnetic resonance or electron spin resonance techniques. A 9 GHz spectrometer has been employed in this work.

Impurity helium solids provide an ideal medium for the study of tunneling exchange chemical reactions in which deuterium atoms interact with H₂ molecules to form HD plus a free hydrogen atom. A subsequent slower reaction involves a deuterium atom interacting with an HD molecule to form D₂ plus a free hydrogen atom. These chemical reactions were

studied by electron spin resonance experiments which took advantage of the fact that the signatures for D and H atoms are entirely different. As the reactions proceeded, the concentration of H atoms grew at the expense of the D atom population when impurity-helium solids containing H, D, H₂, HD and D₂ were studied. Tunneling chemical reactions can occur at liquid helium temperatures, in contrast with ordinary thermally activated chemical reactions which typically require much higher temperatures to produce an observable reaction rate. The negligible temperature dependence for tunneling reactions comes about because they are purely quantum mechanical processes. In this work tunneling does not require that potential energy barriers must be surmounted for a reaction to proceed. Instead, tunneling allows a reactant to pass through such a potential barrier. Tunneling reactions provide an efficient means of producing rather large H atom concentrations.

BACKGROUND.

Systems involving impurity atoms or molecules embedded in inert matrices have fascinated physicists and chemists for many years. The demand for high energy rocket fuels in the late 1950's provided an important stimulus to research in this area. A strong program led by the late Herbert P. Broida was established during this period at the National Bureau of Standards (now N.I.S.T.) in Washington, D.C., USA to investigate free radicals trapped in various matrices. Energy storage for long periods of time was made possible by the inert matrices, which served to isolate the individual free radicals from one another thereby preventing or at least vastly inhibiting chemical recombination. A great deal of emphasis was placed on studies of the free radical atomic nitrogen. The reaction between nitrogen atoms to form nitrogen molecules is the most energetic of all chemical reactions (9.8 eV per N₂ molecule formed). Other free radicals were also investigated including atomic hydrogen. A number of other laboratories became involved in these studies, the results of which were summarized in a book edited by Bass and Broida [1]. Techniques employed included optical spectroscopy, electron spin resonance, thermal measurements and a.c. magnetic susceptibility. Free radicals were created either by gaseous electrical discharges or by X-ray radiation. The former method was most useful when large free radical concentrations were desired. The contents of the electrical discharge tube were cryopumped into a cold finger cooled externally by liquid helium. The sample consisted of a white, snow-like solid. If

nitrogen atoms were present, the sample would emit green light, which corresponded to the decay of a metastable excited state of atomic nitrogen formed in the discharge. In this early work, a number of experiments were performed with nitrogen atoms embedded in a matrix of solid molecular nitrogen. Unfortunately only very low concentrations of atomic nitrogen free radicals were obtained ($\leq .1\%$, far too low for any possible energy storage or rocket fuel applications). Calculations by Jackson [2] performed at the time gave every indication that chain reactions involving recombination would block any attempts to achieve higher concentrations. As time passed, scientists turned to more promising areas of research.

It took more than twenty years for the next major breakthrough to occur in this field. In 1974, E. B. Gordon, L. P. Mezhov-Deglin and O. F. Pugachev [3] in Chernogolovka, Russia invented an entirely new approach to the problem of sample preparation. The basic idea is that gas consisting of a mixture of helium gas and an impurity gas such as atomic and molecular nitrogen was injected into superfluid helium. Much later it was established that a solid formed which was made up of helium and the impurity or clusters of impurities [4, 5]. It is well known that liquid helium solidifies only at pressures of 25 bar or above. The solid formed in the Chernogolovka experiments at the saturated vapor pressure of helium is thought to be composed of the impurity molecules surrounded by thin layers of solid helium. These solids, known as impurity-helium or Im-He solids, are held together by Van der Waals forces. It is now believed that these solids form porous structures similar to aerogel, where the pores or interstices contain superfluid ^4He . The "backbone" of these solids consisted of the impurities surrounded by thin layers of solid helium. The thin solid helium layers around free radical impurities play a strong role in reducing the recombination rate. The Chernogolovka group also found that when the liquid helium was drained out of the pores, the resulting "dry solid" still maintained its integrity. These new solids have been providing a rich new laboratory for the investigation of atomic or molecular species isolated by helium.

The group at Chernogolovka has been investigating impurity-helium solids for about twenty years. They have studied solids with rare gas impurities (Ne, Kr), molecular nitrogen and deuterium impurities, and atomic nitrogen, hydrogen and deuterium impurities. The most powerful methods for studying impurity-helium solids are optical spectroscopy and electron paramagnetic resonance (electron spin resonance or ESR). The former technique has been particularly useful for observing impurity-helium solids containing atomic nitrogen [6, 7]. We recall that the early measurements at the National Bureau of Standards observed

a green glow emanating for hours from atomic nitrogen radicals trapped in a solid N_2 matrix, for example. The detailed spectrum can provide information on the exact location of the nitrogen atoms relative to the components of the trapping matrix (in this case solid N_2). In the Chernogolovka experiments, a truly spectacular display resulted when the $N-N_2$ -He solid is warmed up to temperatures well above the normal boiling point (nbp) of liquid helium. In this case, we are dealing with a dry solid after all the liquid helium has evaporated. As the temperature increases, the diffusion rate of the nitrogen atoms increases. At about 8 K the onset of rapid recombination is manifested by a sequence of bright flashes, indicating that explosive chemical reactions are taking place [8]. Transient spectroscopy could provide considerable detail regarding the kinetics of these explosive events.

Electron spin resonance (ESR) techniques can be used to study any free radical (atomic or otherwise) with an unpaired electron spin. This method is particularly useful for determining the actual free radical content of the sample. The Chernogolovka group performed a series of ESR studies on impurity helium solids containing atomic nitrogen, deuterium and hydrogen impurities [4, 9, 10]. Inevitably the solids also contained N_2 , D_2 and H_2 molecules respectively in addition to the solid helium. As a result of hyperfine interactions and differing nuclear spins and magnetic moments, each of the three atomic species has a unique ESR signature. The Chernogolovka observations revealed that very high concentrations of atomic nitrogen could be stored in the $N-N_2$ -He impurity helium solids [4, 5]. The results were obtained by comparing the observed ESR signal with that of a sample of DPPH with a known number of total spins. It was found that $[N]/[N_2]$, the relative concentration of nitrogen atoms, could be as large as 50%. It was therefore possible to obtain total spin densities as high as $4 \cdot 10^{20}$ per cubic centimeter. The atomic nitrogen concentrations obtained in the impurity-helium solids were orders of magnitude higher than those achieved in the early experiments in the 1950's in the United States and well above Jackson's theoretical prediction. The energy storage was comparable to the best chemical explosives for the highest radical concentrations produced in the impurity-helium solids.

The ESR technique was also applied to a number of other impurity solids at Chernogolovka, including those involving atomic deuterium and/or atomic hydrogen impurities. The most fascinating result was an observation made on a solid initially containing hydrogen atoms, hydrogen molecules, deuterium atoms and deuterium molecules. It was found that the concentration of hydrogen atoms was considerably larger than the concen-

tration of deuterium atoms in spite of nearly equal concentrations of D_2 and H_2 in the make-up gas [9]. This observation was attributable to the occurrence of chemical reactions in which the hydrogen atom population increased at the expense of a lower deuterium atom population.

A program to investigate impurity-helium solids was initiated at Cornell University in early 1998. Prior to this time our co-worker, Vladimir V. Khmelenko, had been deeply involved in the Chernogolovka research mentioned above. In the 1980's, David M. Lee participated in experiments by the Cornell Low Temperature group on spin polarized atomic hydrogen gas, which culminated in the discovery of nuclear spin waves in this rarefied gas [11]. The Cornell research program on impurity-helium solids began with ultrasound studies to obtain information on the structure of these highly porous materials. The results were consistent with an aerogel-like structure. Aerogel permeated with superfluid ^3He or ^4He has been a subject of study at Cornell for many years. This experience was quite valuable in the interpretation of our ultrasound data.

X-ray diffraction experiments performed at the Brookhaven National Laboratory Light Source by our group, as part of a collaboration, provided further information regarding the structure of impurity-helium solids. The aggregation of the impurities into larger clusters was observed in both the X-ray and the ultrasound experiments as the samples were heated above the lambda temperature of liquid helium [12].

Magnetic resonance studies have been under way at Cornell for the past three years. The main results have come from electron paramagnetic resonance studies of nitrogen atoms, deuterium atoms and hydrogen atoms in the impurity helium solids. Some preliminary nuclear magnetic resonance experiments were also performed on an impurity-helium solid containing molecular deuterium.

SAMPLE PREPARATION

The most crucial element required for experiments on impurity-helium solids is the apparatus for sample preparation. The breakthrough by Gordon, Mezhov-Deglin and Pugachev at Chernogolovka has made it possible to collect samples containing copious amounts of free radicals.

In our work we used a variation of the Chernogolovka technique [5]. A schematic diagram

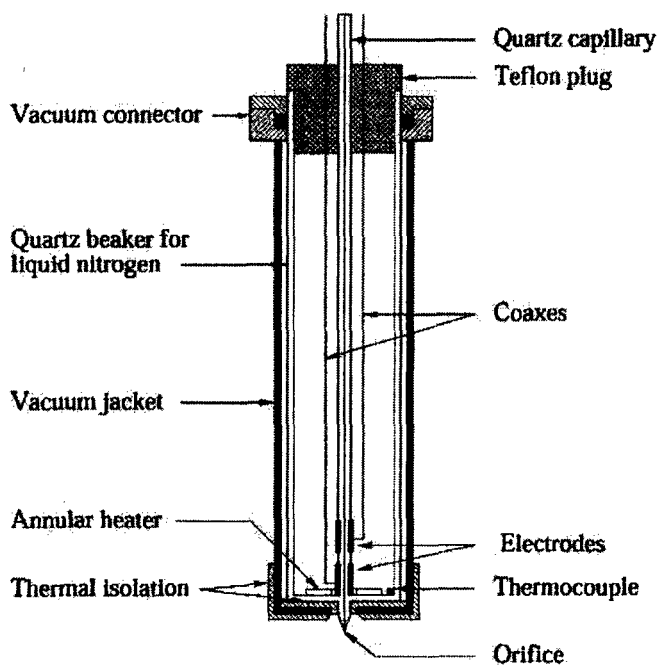


FIG. 1: Diagram of the source of atoms and molecules used for preparation of Im-He solids.

of our sample source is shown in Fig. 1. A fused quartz capillary is cooled by liquid nitrogen contained in an outer quartz tube concentric with the capillary. Two electrodes placed in the liquid nitrogen each surround the capillary. 60 MHz radiofrequency voltage is applied between the two electrodes when the sample gas is fed through the capillary. The products of the discharge, including any undissociated molecules, emerge from the bottom of the capillary through a nozzle with a one millimeter diameter orifice. The whole source assembly is surrounded by a double walled stainless steel tube with the region between the inner and outer walls being evacuated to thermally insulate the quartz tubes containing the liquid nitrogen and the sample from the external liquid bath. The lower portion of the assembly is placed in a liquid helium dewar, with the liquid helium level always below the nozzle. Since the sample gas consisted of a mixture of helium and the impurity, it was necessary to prevent freezing out of the impurities in the nozzle, which would give rise to a blockage. This was accomplished by placing an annular heater ($R \approx 10\Omega$) at the lower end of the capillary. The various gases constituting a sample are stored and mixed in a gas handling system at room temperature (300 K). The sample is then fed into the inner capillary and through the

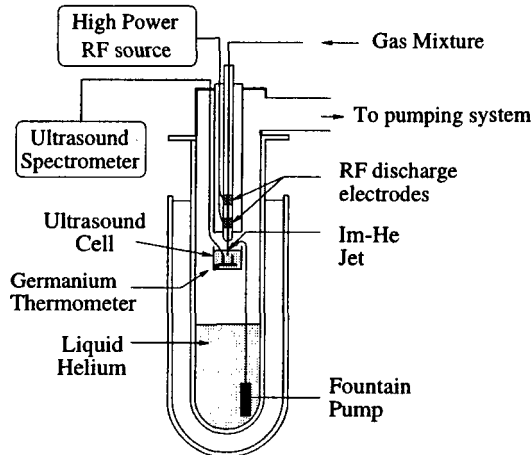


FIG. 2: Experimental setup for preparation of Impurity-Helium solid samples for ultrasound studies.

radiofrequency discharge before emerging from the orifice, as discussed above. The sample gas beam is aimed at the center of a small collection beaker a few cm below the orifice. The beaker is kept full of superfluid helium via a fountain pump which transfers liquid to the beaker from the main helium bath whose level is 20 cm below the collection beaker. This compensates for any helium which evaporates during the heating associated with the sample collection procedure. The main bath temperature is held at 1.5 K with the aid of powerful pumps. When the sample is being collected, a small depression appears at the liquid surface just below the nozzle from which the beam emanates. As it exits the nozzle, the beam is clearly visible as a result of light produced from the decay of excited states formed in the discharge. The overall arrangement is shown in Fig. 2. As the gas passes through the helium surface, a snow-like solid forms which then sinks to the bottom of the beaker. The "snow flakes" then congeal into a translucent solid corresponding to the impurity-helium solid sample. For the case of a sample containing atomic nitrogen the solid glows with the characteristic green color first seen in the National Bureau of Standards optical spectroscopy experiments. This green light, which persists for several hours, is associated with spectral lines from the decay of the $^2D \rightarrow ^4S$ metastable states of atomic nitrogen.

In our recent studies, we have been investigating the structure of the porous Impurity-Helium solids by means of ultrasound propagation through liquid helium contained in the pores (work performed at Cornell University) and via X-ray diffraction studies (work con-

ducted at the Brookhaven National Laboratory Light Source). This work is a part of ongoing investigations of Impurity-Helium solids at Cornell University [13, 14] and Brookhaven National Laboratory [12, 15, 16]. A paper summarizing the collaboration between our group at Cornell and workers at Rutgers, Chernogolovka, and the Max-Planck Institute in Stuttgart appeared in the *Phys. Rev. B* in January 2002 [12]. The results of both techniques have indicated that at the formation of the sample at 1.5 K the impurity entities are either individual impurity atoms or most likely several impurity atoms bound together by Van der Waals forces. As the samples warm, diffusion takes place both for helium atoms in the surrounding coatings and for the impurities themselves. The impurity clusters slowly grow in size. This effect is enhanced by release of the heat of aggregation of the impurity clusters which, for the sake of discussion, is taken to be the same order of magnitude as the latent heat of melting of bulk samples of the impurity.

A dramatic increase in the growth rate of the impurity clusters is expected to occur for temperatures above the superfluid transition T_λ because the thermal conductance of liquid helium in the pores becomes dramatically smaller as the sample is heated through T_λ . Thus the heat of aggregation can lead to local hot spots which contribute to higher diffusion rates in these localized regions, a situation which is favorable to the formation of larger impurity clusters. It is therefore to be expected from this crude model that heating the sample above T_λ and then cooling back through T_λ would lead to irreversible changes. As we shall see, this is exactly what has been observed in the experiments. The expected time evolution according to this model for a sample is shown in Fig. 3.

For the case of atomic free radical impurities, the very large amount of heat released during molecular recombination enhances the effects described above. Recall that for very high concentrations of free radicals, the sample will spontaneously explode. In the following sections we present ultrasound data and X-ray diffraction data from our experiments. These recent results are consistent with the qualitative description discussed above.

ULTRASOUND AND X-RAY DATA.

We shall first discuss the ultrasound experiments performed by the Cornell group. The impurity helium sample was formed in a sound cell (shown in Fig. 4) which consisted of a pair of quartz (1 MHz fundamental) or lithium niobate crystal transducers separated by

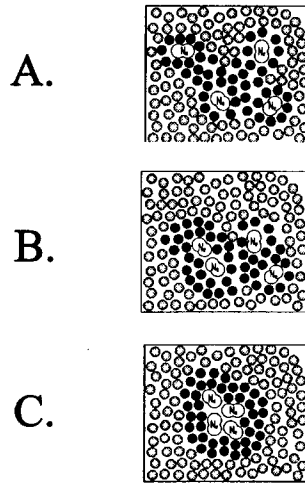


FIG. 3: The model of Im-He solid formation: A. On formation, the impurities are mainly isolated from one another by helium atoms in the solid (black circles). Superfluid liquid helium contained in the pores (gray circles) transports heat efficiently. B. As the sample is warmed up, diffusion allows impurities to aggregate slowly. The associated heat is carried away by superfluid helium. C. As the sample is warmed above the T_λ , the diffusion rate increases. Larger aggregates form. The heat of aggregation can no longer be carried away by liquid helium for $T > T_\lambda$. More diffusion takes place and even larger aggregates form.

a distance of 1.5 cm. The sound cell was placed in the collection beaker. Transparent deflecting shields were placed above the cell to channel the Im-He solids into the sound propagation path. The transducers were often operated at the odd harmonics 3 MHz and 5 MHz. A pulse-time-of-flight method was used to measure the velocity and the attenuation of the sound as it traversed the sample, which consisted of a porous aerogel-like solid with the pores being filled with liquid helium. The sound propagated mainly through the liquid helium in the pores as evidenced by the fact that the sound velocity was very close to that of bulk liquid helium. The attenuation of sound on the other hand, was greatly influenced by the presence of the porous impurity-helium sample. The attenuation results were indeed dependent on the history of the sample, as expected from the qualitative model presented previously.

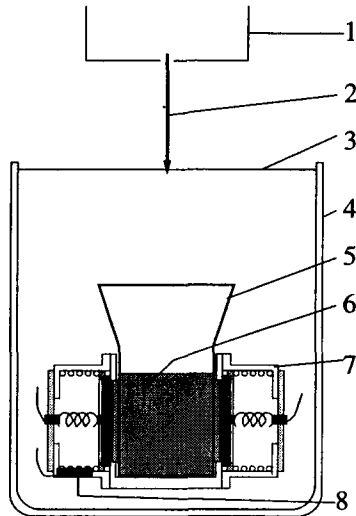


FIG. 4: Experimental cell: 1 - Atomic and molecular source, 2 - Impurity-Helium jet, 3 - surface of liquid helium, 4 - quartz dewar, 5 - quartz funnel, 6 - Impurity-Helium solid, 7 - ultrasound cell, 8 - germanium thermometer [14].

The next set of figures illustrates this point. Figure 5 portrays sound attenuation results for Kr-He, Ne-He, N₂-He and D₂-He impurity-helium solids. The sequence of events during the warm up of a sample involves successive decoupling of the normal fluid component from the walls of successively smaller channels as the viscous penetration depth decreases with increasing temperature according to $\delta_{visc} = (2\eta/\omega\rho_n)^{1/2}$. Here η is the viscosity, ω is the angular frequency of the sound and ρ_n is the normal fluid density which increases with temperature according to the two-fluid model. This increased freedom for the normal fluid to flow dissipatively as the temperature rises leads to a concomitant increase in the sound attenuation as shown in Fig. 5. A plateau is eventually reached where sound propagates mainly through the largest channels, a process which can be thought of as sound propagation through bulk liquid helium.

It is noteworthy that the samples containing heavier impurities tend to have a considerably higher sound attenuation, ranging from the lightest solid sample D₂-He with an attenuation close to that of bulk liquid helium to the heaviest, Kr-He which has the highest attenuation. For the case of the D₂-He solid, a possible interpretation is that the D₂-He solid has almost the same density as that of bulk superfluid helium, so that sound propagation will be relatively unimpeded due to the close matching of the acoustic impedances.

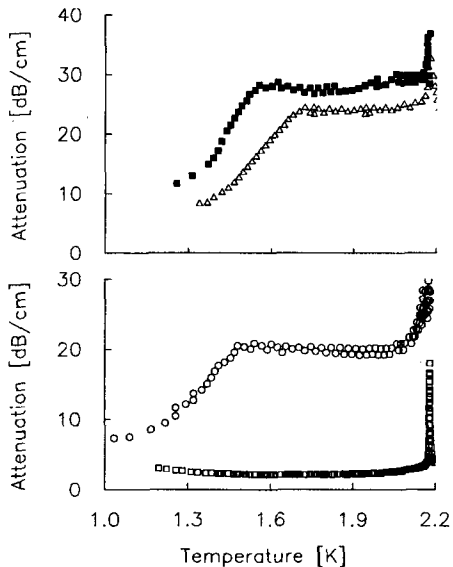


FIG. 5: The behavior of ultrasound attenuation in liquid helium confined in different impurity-helium solids: (a) in Kr-He solid (solid squares), in Ne-He solid (triangles); (b) in N_2 -He solid (open circles), in D_2 -He solid (open squares).

The acoustic impedance becomes more mismatched with increasing impurity mass, leading to higher attenuation. The small oscillations of attenuation seen in some of the heavier samples as shown in Fig. 5 appear to be a property of sound propagation through the macroscopic channels in the sample. The period of the oscillations tends to become shorter as the lambda temperature is approached which is consistent with a possible interference effect involving bulk channels. Much more work will be required before a full explanation of these oscillations can be provided.

Figure 6 illustrates the history dependence of the sound attenuation as the impurity-helium samples are heated and then cooled. If the heat is applied until the sample is warmed above the lambda temperature, an irreversible change takes place which is manifested by a considerably higher attenuation as the sample is cooled below the lambda temperature. If the sample is heated to a point just below the lambda temperature and then cooled down the attenuation behaves reversibly. We believe that these results show that larger clusters of impurities are formed at temperatures above the lambda point as described in our qualitative picture. These larger (and therefore heavier and denser) impurity clusters give rise to a larger attenuation as shown in Fig. 6, where data for N_2 -He samples, D_2 -He

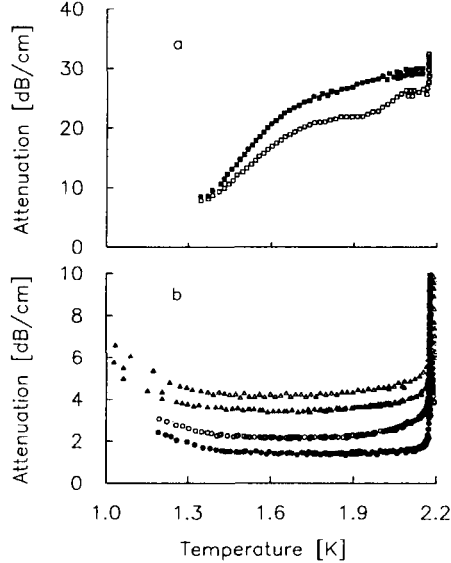


FIG. 6: The attenuation of ultrasound in liquid helium: (a) in N_2 -He solids [after preparation (open squares), after crossing λ -point and cooling down (solid squares)]; (b) in bulk helium (solid circles), in D_2 -He and D - D_2 -He solids [after preparation of both solids (open circles)], after crossing λ -point and cooling down D_2 -He (solid triangles), after crossing λ -point and cooling down D - D_2 -He (open triangles).

samples and D_2 -He samples containing atomic deuterium are represented. This latter sample exhibits an even higher attenuation increase after heating and cooling through the lambda point as a result of additional heat generated via recombination of deuterium atoms into D_2 molecules.

The ultrasound experiments also furnish information on the characteristic pore size in these porous impurity helium solids, where we point out that the pore sizes actually extend over a range of values, in analogy with light aerogels. The key parameter needed to describe the behavior of sound attenuation in liquid ^4He in porous materials is the viscous penetration depth. In superfluid helium, the normal fluid fraction changes from nearly zero to unity between 1.0 K and 2.17 K, causing δ_{visc} to change from 1500 nm to 100 nm for 5 MHz sound. As a sample of superfluid ^4He contained in the pores of our impurity helium solid is cooled, the viscous penetration depth increases, so more and more of the fluid is locked to the walls. Therefore, at the lowest temperature, where almost complete locking occurs, dissipative sloshing of the normal fluid through the pores is minimal. The attenuation thus

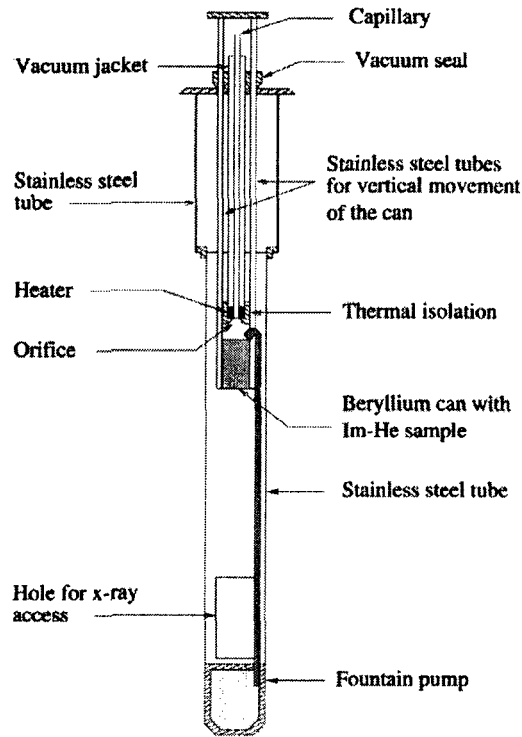


FIG. 7: The diagram of insert for a variable temperature Oxford cryostat. The access hole for X-rays also allows entry of liquid He from the main bath.

decreases as the sample is cooled. This effect is quite evident for temperatures below a crossover temperature of about 1.5 K (depending on sample and sound frequency). Above this temperature, the attenuation is so large that sound propagates relatively freely only in the very largest (macroscopic) channels where bulk helium behavior is observed, corresponding to a saturation of the attenuation above the crossover temperature. By calculating the viscous penetration depth at this temperature, we can find the corresponding pore size which for our samples ranges from 200-800 nm. The very smallest pores were studied by observing the attenuation at T_λ . The smallest pores were about 8 nm. This type of analysis plus the fact that the sound velocities are always nearly equal to that for bulk liquid helium provides very convincing evidence that we are dealing with highly porous materials. A more complete discussion of these effects is given in [12, 14].

Information obtained from the x-ray measurements [12, 16] was consistent with the ultrasound results. The impurity-helium solids were placed in the path of the synchrotron

radiation x-ray beam at the Brookhaven National Laboratory light source. Experiments were performed with 17.3 keV x-rays (beam line X20B) for Ne-He samples and with 8 keV x-rays (beam line X20A) for all other samples. Figure 7 shows a diagram of the variable temperature x-ray cryostat insert used in these experiments. The samples were contained in a beryllium can which was lowered into the path of the x-ray beam. Since the impurity-helium samples were random in nature, powder pattern diffraction peaks were measured. Broad diffraction peaks correspond to very small clusters whereas narrow diffraction peaks correspond to larger nanocrystallites, since more crystal planes are available to scatter the incident x-rays giving rise to sharper diffraction patterns. The action of diffusion in the impurity-helium solids is expected to lead to the formation of larger crystallites. Immediately following the preparation of impurity-helium samples, cluster peaks were not observed, in almost all cases. Only for the case of Ne-He samples was a very broad neon cluster peak observed upon formation of a Ne-He solid sample. As the sample was heated above the lambda temperature the neon cluster peaks became higher and narrower, exactly as one would expect when larger crystallites formed as a result of diffusion. The diffraction angles of the observed peaks corresponded to peaks expected for solid neon. Figure 8 shows a set of peaks corresponding to different temperatures as the Ne-He sample was warmed from 2.5 K to 4.2 K. The sample was always surrounded by liquid helium for this set of measurements.

For the other impurity-helium solids, the results can be described as follows: After heating the Im-He samples up to 4 K, broad impurity cluster peaks were observed for D₂-He, N₂-He and the mixed sample D₂-N₂-He. Evaporating liquid helium from the cell led to the creation of relatively large impurity microcrystallites. Diffraction peaks corresponding to these larger crystallites became higher and narrower as the temperature increased above 4 K in these "dry" solids. As discussed above, the larger crystallite sizes were corresponded to smaller widths as is normally the case in x-ray diffraction. A careful analysis is discussed in [12]. Typical sizes ranged from 30 Å to 80 Å.

Finally, Fig. 9 shows a N₂-He impurity solid result in which the sample was always surrounded by liquid helium. The lower trace gives the signal at 1.5 K before warming to 4 K. The signal is indistinguishable from that of the helium background which has not been subtracted. After heating the sample to 4 K and cooling it back to 1.5 K a broad nitrogen peak was observed, as indicated by the upper trace. This result again illustrates the growth of nanocrystallites as a result of warming the sample through the lambda temperature.

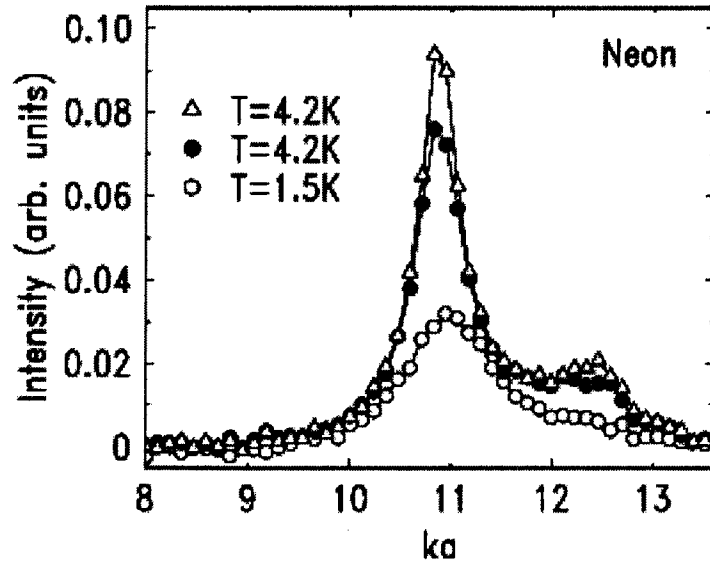


FIG. 8: X-ray diffraction patterns for the Ne-He samples immersed in liquid helium at $T=1.5\text{ K}$ and $T=4.2\text{ K}$. Liquid helium signal is subtracted. k is momentum transfer, a is the lattice constant of solid Ne. The lower curve at $T=4.2\text{ K}$ was taken immediately after the sample was warmed up. The higher curve at $T=4.2\text{ K}$ was taken 15 min afterwards.

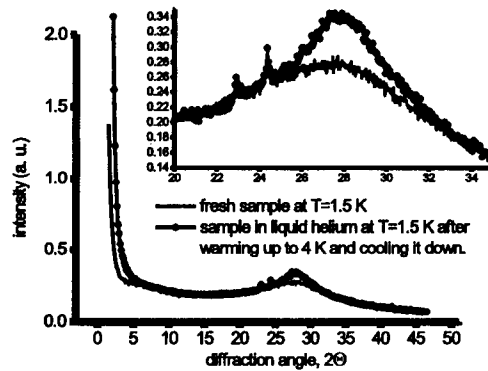


FIG. 9: X-ray diffraction patterns ($E = 8\text{keV}$) from the $\text{N}_2\text{-He}$ solid immersed in liquid helium, where helium background is included. The inset shows the signal on a finer scale.

Two different types of measurements, ultrasound and x ray studies, have shown that diffusion gives rise to the formation of tiny crystallites of the impurity as samples of impurity-

helium solids are warmed up through the lambda temperature of liquid helium. Further experiments and theoretical studies are required to progress from the qualitative ideas presented herein to a quantitative understanding.

The importance of this work is that it shows quite clearly the necessity of maintaining the impurity-helium solids at temperatures below the lambda temperature to prevent excessive recombination for the free radical impurities and structural changes in all samples. This is especially significant for purposes of any applications requiring energy storage.

NMR STUDIES OF IMPURITY-HELIUM SOLIDS

Nuclear magnetic resonance (NMR) is an extremely versatile technique which permits measurements of spin diffusion and relaxation processes, mainly by means of pulse methods. It should be primarily useful in studies of H_2 and D_2 molecules in the impurity helium solids. The technique suffers from the disadvantage that nuclear moments are rather small. This, combined with the dilution of spins found in impurity helium solids leads to the expectation that serious signal to noise problems might be encountered. The problem is further exacerbated in H_2 samples because of the Pake doublet splitting associated with the intramolecular dipole-dipole interaction in the $J=1$ orthohydrogen. This kind of interaction is a much more manageable problem in the case of deuterium for which the nuclear dipole moment is about one sixth that of hydrogen.

In our experiments, success was finally achieved in a deuterium helium impurity solid studied by means of a CW resonance spectrometer operating at 3.66 MHz with lock-in detection. The only way signals could be obtained was by increasing the ratio of deuterium to helium in the make up gas. Make up gas for this sample consists of D_2 - He in ratio 1:10. No signal was observed shortly after the initial formation of the D_2 helium solid. It was only possible to see a signal when the sample was heated well above the lambda temperature of liquid helium (see Fig. 10). We concluded that it was necessary to form small crystallites before a signal could be observed. The lack of a response at the lowest temperatures is perhaps attributable to saturation with the longitudinal relaxation time being too large for isolated deuterium molecules immediately following sample preparation. This saturation became a much less serious problem as small crystallites of solid deuterium formed in the sample as a result of diffusion at the higher temperatures. Nevertheless, in spite of our best

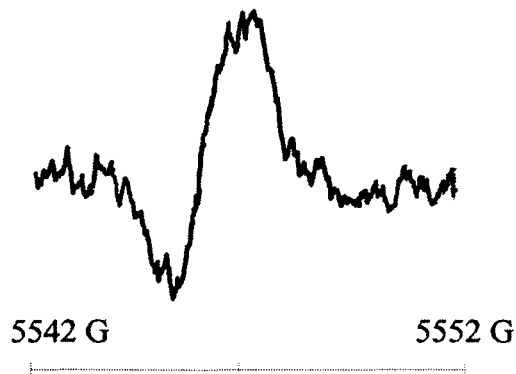


FIG. 10: NMR signal from D_2 -He solid after it was heated well above T_λ and cooled down to $T=1.5$ K ($f=3.66$ MHz).

efforts, we were never able to achieve satisfactory signal to noise ratios to perform reliable quantitative measurements.

We are forced to the conclusion, on the basis of these experiments, that NMR experiments in these impurity helium solids must be carried out at much higher fields to provide enhancement of the signal to noise ratio as a result of a more favorable Boltzmann factor and higher sensitivity.

ELECTRON SPIN RESONANCE STUDIES OF IMPURITY-HELIUM SOLIDS

An important set of electron spin resonance (ESR) studies were carried out at Chernogolovka on impurity helium solids [4, 9, 10]. At our laboratory at Cornell, we have recently investigated the ESR spectra of the nitrogen impurity-helium solid and solids involving atomic hydrogen and atomic deuterium impurities [17]. Since the electronic moments are quite large, in contrast with nuclear moments, very large signals can be observed as a result of the large transition frequencies associated with spin flips, and the correspondingly large Boltzmann factors. Thus it is possible to investigate small, dilute samples. If the steady magnetic field is sufficiently homogeneous, ESR lines corresponding to transitions between various hyperfine states can easily be resolved. For the case of high spin densities, however, the dipole-dipole interaction can lead to enough line broadening to prevent resolution of the

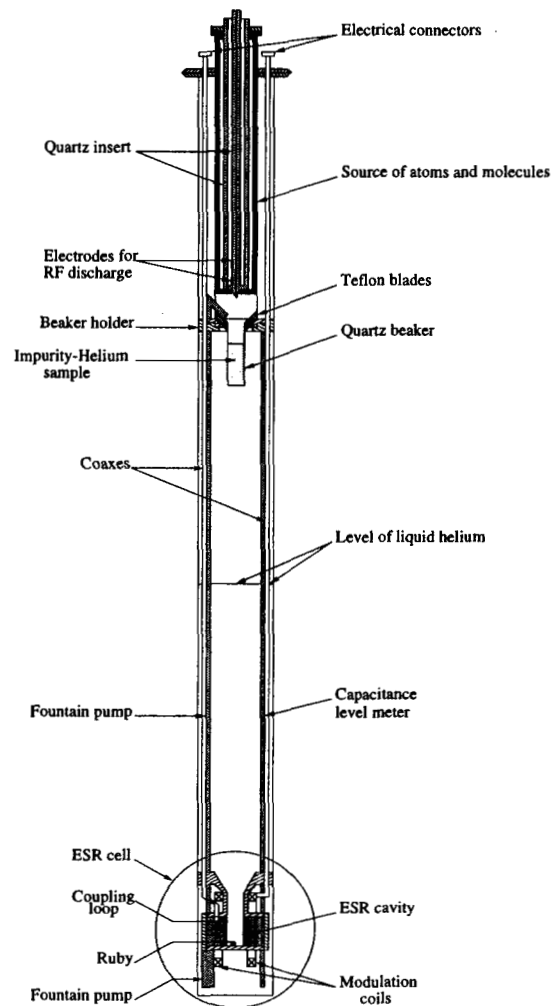


FIG. 11: Low temperature insert for Im-He sample preparation and ESR investigations. The quartz beaker is lowered into the ESR 9.07 GHz TE_{011} resonant cavity for measurements after sample preparation.

hyperfine lines.

In our experiments at Cornell, we have employed a continuous wave (CW) 9 GHz microwave spectrometer. An electromagnet provided a homogeneous steady field H_0 up to 10 kG. The homogeneity was determined via the nuclear magnetic resonance signal from a water sample. A cylindrical TE_{011} resonant cavity (see Fig. 11) operating in the reflection mode was positioned in our metal cryostat near the midpoint of the magnet pole pieces. The cylindrical axis of the cavity was aligned vertically. A hole through the center of the

top of the cavity allowed the sample to be inserted. The central position of this hole ensured that the sample would be placed in the maximum microwave magnetic field H_1 . The hole had a minimum effect on the operation of the cavity, since the electric field at this position was minimized for the TE_{011} mode. Microwaves were generated by a klystron and then routed to the cavity by a circulator. The signal reflected from the cavity was sent by the circulator to the receiver which consisted of detectors and an amplifier chain. The magnetic field at the position of the cavity was modulated by a pair of coils attached to either side of the cavity. The coils generated a 100 kHz alternating magnetic field. Data was taken as the magnetic field of the large electromagnet was swept slowly through the ESR lines. The modulation field was kept small enough to produce an undistorted derivative of the ESR signals, but large enough to provide an adequate signal level. The signal leaving the detector was dominated by the modulation frequency. This signal was amplified and then fed into a lock-in amplifier which greatly enhanced the signal to noise ratio. The output of the lock-in detector was displayed on a chart recorder trace and was also recorded in a computer to allow for rapid data processing. The actual spectral lines were obtained by integration of the derivative signals obtained in this way.

A small ruby crystal, mounted inside the resonant cavity, provided a comparison signal to help calibrate the amplitude of the sample signal. The sample and the ruby are expected to vary in the same way as the temperature fluctuates or the spectrometer sensitivity drifts. The ruby can in turn be calibrated against a known sample of DPPH to enable us to determine the absolute number of spins in our samples. The ESR lines of ruby are highly dependent on the orientation of the crystal. An orientation was chosen so that the ruby signals do not overlap the signals produced by samples.

The microwave power entered and exited the resonant cavity through a small 50Ω coaxial cable connected to a small coupling loop constructed from a single turn of Cu wire. At the top of the cryostat, the coaxial cable was connected to the X-band wave guides of the bridge. Typically 5 microwatts of microwave power were delivered to the resonant cavity. The cable lengths were tuned so that the output of the circulator was significant only when an ESR line was being traversed as the field of the electromagnet was varied. The impurity-helium samples were formed in a special beaker which consisted of a small quartz tube closed off at the bottom. A quartz funnel was attached to the top of the tube to collect the sample gases as they emerged from the orifice. A pair of rotating teflon blades was employed to sweep

any of the impurity-helium solid that might have stuck to the funnel into the lower portion of the sample tube.

During the collection procedure the sample cell beaker was placed high in the cryostat, just underneath the orifice. The beaker was kept full of liquid helium by the fountain pump, as discussed earlier. The sample cell was then lowered into the main superfluid bath and then into its final position with tube corresponding to the lower end of the sample positioned inside the resonant cavity.

The atoms being studied in our ESR investigations are nitrogen, deuterium and hydrogen. The value of H_0 employed in these experiments places us close to the high field regime of the Breit-Rabi formula. Therefore a small shift of the observed spectra from the high field limit is expected and is seen in the data. The simplest spectrum is obtained for hydrogen atoms because the proton and the electron are each spin $1/2$ objects. This leads to four possible spin states. The selection rules for magnetic dipole transitions give two hyperfine lines in the ESR spectrum of hydrogen. The large proton moment leads to a very large splitting (508 G) between these lines. The deuterium ESR spectrum has three lines, almost equally spaced (the departure from equal spacing corresponds to the value of H being slightly below the high field limit). The triplet structure comes about as a consequence of the deuterium spin being $I=1$. The deuteron magnetic moment is smaller than that of the proton so that the splitting between components of the triplet is smaller than the hyperfine splitting for the case of the atomic hydrogen doublet (76.7 G and 78.7 G). Atomic nitrogen also has three hyperfine lines in its ESR spectrum. The nitrogen splitting (4.2 G) is more than an order of magnitude smaller than that for deuterium. Hence for the case of impurity helium solids with high nitrogen atom concentrations the line broadening associated with the dipole-dipole interactions makes it more difficult to resolve the individual hyperfine lines.

Preliminary ESR measurements were performed on atomic nitrogen in a $N-N_2$ -He impurity helium solid. In Fig. 12, we show the derivative signal for ESR lines obtained for an impurity helium solid with a moderate relative concentration of nitrogen atoms. The characteristic triplet structure is present, but the three individual lines are not well separated. Better resolution was obtained when more dilute samples were measured. The nitrogen results were very similar to those obtained at Chernogolovka at a much earlier date [4, 5]. These measurements were used mainly to develop our experimental procedures, since it is much easier to obtain very large free radical concentrations for atomic nitrogen.

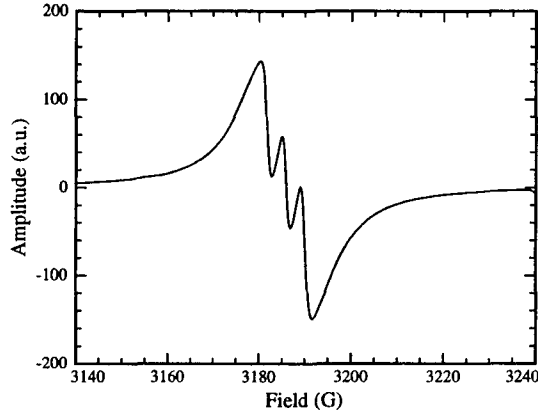


FIG. 12: ESR spectrum of nitrogen atoms in N_2 -He solid ($f = 9.07$ GHz) at $T = 1.43$ K. The poor resolution results from the dipole-dipole interaction between the N atoms.

We have recently obtained new results in impurity helium solids containing H, D, H_2 , and D_2 . In Fig.13a, the main features of the atomic hydrogen and deuterium derivative spectra of a sample prepared from an initial gas mixture in the ratio of $H_2:D_2:He = 1:4:100$ are shown. We observe the allowed hyperfine transitions of H and D atoms [18] as well as a small forbidden line of the hydrogen atom which involves a simultaneous spin flip of the electron and proton. Magnetic dipole selection rules for allowed electron spin flip transitions require the microwave field in the cavity H_{rf} to be perpendicular to the applied steady field H . For observation of the forbidden line we need $H_{rf} \parallel H$ [19]. This condition is easily met in our experiment because we operate with macroscopic samples occupying a considerable part of the cavity, including areas with significant components $H_{rf} \parallel H$ (especially at the top and the bottom of the cavity). The intensity (corresponding to the area under the absorption line) of the forbidden line is about 200 times smaller than the allowed hydrogen line, roughly in accord with theory [19].

Both the deuterium and the hydrogen ESR lines are accompanied by two satellite lines, one on either side of the main line (Fig.13 b,c). Satellite lines have been previously observed for H and D atoms contained in solid hydrogen by Miyazaki *et al.* [20]. The atoms were produced in very low concentrations by γ -irradiation of solid H_2 , solid HD and solid D_2 . The satellites are associated with forbidden ESR transitions involving an electron spin flip of a hydrogen or deuterium atom and simultaneous spin flip of protons on neighboring HD

or ortho hydrogen molecules [20], simply as a result of dipolar coupling.

Each of the ESR signals was fitted with a sum of three Gaussians (allowed line plus two satellites). From these fits, shown in Fig.13(b,c) by solid lines, the ratio of the intensities of the satellite and main lines are found to be 0.12 ± 0.02 . Even if the intensities of these lines change with time, the ratios remain constant. The separations between the main and the satellite lines have also been obtained from the fits. These splittings (4.5 ± 0.1 G) are consistent with proton spin flips in a 3 kG field. Analogous splitting for electron spin-deuteron spin interactions is only 0.7 G, unobservable in our experiments because the ESR linewidths are about 2 G.

The measured ratio of intensities has been compared with the expression obtained by Trammell *et al.* [21]

$$I_{\text{satellite}}/I_{\text{main}} = 3/20(g_e\beta_e/H)^2\langle r_n \rangle^{-6}n \quad (1)$$

to find the trapping sites of atomic species in molecular matrices. In the above equation g_e

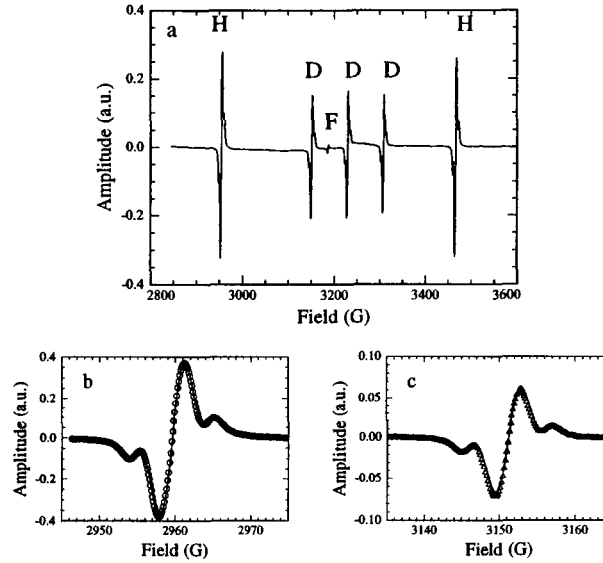


FIG. 13: a. ESR signal from Im-He sample prepared from gaseous mixture $\text{H}_2:\text{D}_2:\text{He}=1:4:100$. 'H' marks allowed ESR transitions between hyperfine levels of atomic H; 'D' indicates the hyperfine transitions in atomic D, and 'F' indicates the forbidden ESR transition of H atoms. At the bottom: Typical derivative signals for low field hyperfine lines of (b) hydrogen and (c) deuterium atoms showing both the allowed and the accompanying satellite lines.

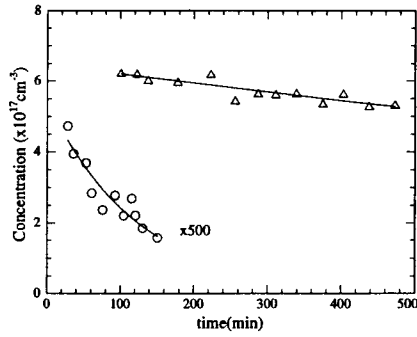


FIG. 14: Time dependence of concentrations of atomic deuterium (prepared from $D_2:He=1:20$ mixture [open triangles]) and atomic hydrogen (prepared from $H_2:Ne:He=1:4:100$ [open circles]) in Im-He solids stored at $T = 1.35$ K.

is the electron g -factor, β_e is the Bohr magneton, H is the applied steady field, $\langle r_n \rangle$ is the average distance from an atom to a proton belonging to a neighboring molecule and n is the number of these protons. This analysis assumes that almost all of the hydrogen atoms or deuterium atoms are close to neighboring molecules. The ratio would be considerably smaller if substantial numbers of totally isolated atoms were present, an entirely conceivable situation for Im-He solids. If we make the reasonable assumption that each atom interacts with one or two protons (from neighboring H_2 or HD), then using eq.1 we find that the average distance between the atom and neighboring proton is 1.9-2.2 Å, which is comparable to the distance between the interstitial sites and the lattice sites in the hcp structure of solid HD or solid H_2 , whose lattice constants are 3.6 Å and 3.8 Å. In the work of Miyazaki *et al.* [20], the H atoms in H_2 matrices were separated from H_2 molecules by 3.6-4.0 Å, whereas for the case of H atoms in HD matrices this distance was 2.5-2.6 Å. The discrepancy between these results and our own may be attributable to the difference in sample composition and sample preparation. Our results provide strong evidence that a large fraction of the hydrogen and deuterium atoms are found in clusters of molecular isotopes of hydrogen.

Estimates of the concentrations of atoms were done by comparing the intensity of the hydrogen and deuterium atomic signals (obtained by double integration of the raw data) with the intensity of signals from a small ruby crystal with a known number of atoms. The latter was placed at the bottom of the cavity. The ruby was calibrated prior to the experimental run against a standard organic compound DPPH with a known number of

spins.

The time dependence of the concentrations of D atoms in D-D₂-He samples (produced from a D₂:He=1:20 mixture) and H atoms in a H-H₂-Ne-He sample (obtained from H₂:Ne:He=1:4:100 mixture) are displayed in Fig.14. The addition of neon was required in the latter sample because, unlike D₂-He samples, the H₂-He solid does not sink to the bottom of the cell, due to its small density. The slow decay of D atoms (with characteristic time $\tau_D = 2500 \pm 500$ min) is attributed to very slow migration of deuterium atoms through molecular deuterium in the clusters ($D+D_2 \rightarrow D_2+D$) until recombination with another D atom occurs ($D+D \rightarrow D_2$). The migration of isolated atoms driven by zero point motion may also play a role although we have no evidence of the presence of atoms with only helium neighbors as yet. Much faster migration ($H+H_2 \rightarrow H_2+H$) can explain the much more rapid decay of the number of hydrogen atoms. The decay time of H atoms shown in Fig.14 is 150 ± 20 minutes, an order of magnitude faster than for the deuterium atoms. Kagan *et al.* [22] have investigated theoretically the difference in decay rates for hydrogen and deuterium atoms, respectively and has found that this difference is not simply a question of mass difference, but rather is determined by differences in phonon processes for the hydrogen and deuterium atom impurities.

The simultaneous presence of deuterium and hydrogen molecules in the make up gas allows us to form impurity helium solids containing hydrogen atoms and deuterium atoms as well as hydrogen and deuterium molecules. In Fig.15(a-c) we show the results of our experiments, which dramatically illustrate the time dependence of the hydrogen and deuterium atom concentrations for different initial make-up gas mixtures [17]. In spite of the higher concentration of D₂ compared with that of H₂ in the sample produced from initial gaseous mixture H₂:D₂:He=1:2:60, the concentration of deuterium atoms is about two orders of magnitude smaller than the hydrogen atom concentration and decays more rapidly (Fig.15a). These results are in sharp contrast to our studies of H₂-Ne-He impurity solids, with no deuterium present, in which the decay of hydrogen atoms due to recombination was much more rapid. The explanation is that when deuterium atoms are present, the supply of hydrogen atoms is replenished via chemical reactions $D+H_2 \rightarrow HD+H$ and $D+HD \rightarrow D_2+H$. Furthermore, these reactions also explain the faster decrease of the deuterium atom concentration as compared to that in our D-D₂-He sample (Fig.14). In Fig.15b the population of hydrogen atoms remains almost constant, meaning that the production is almost in balance

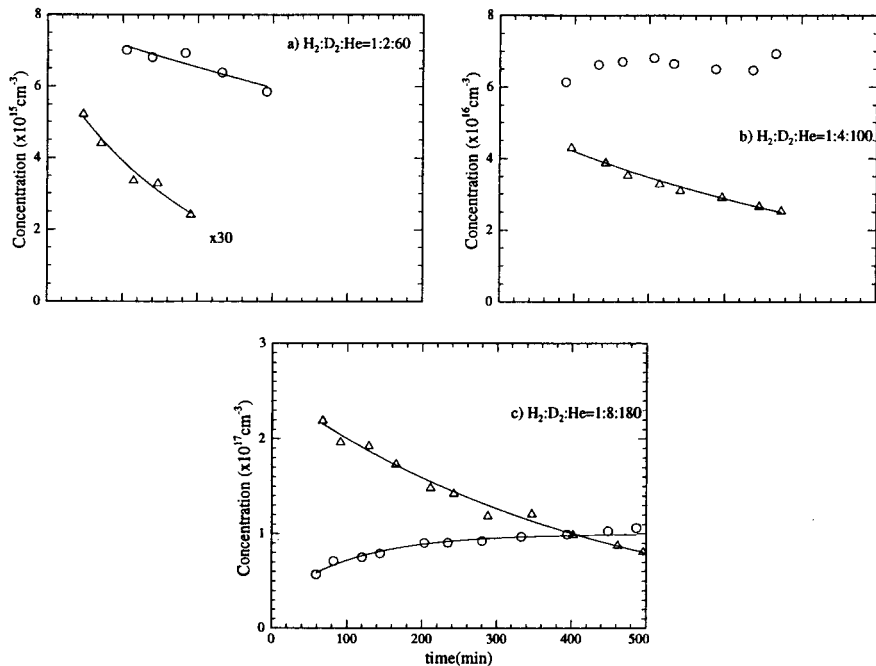


FIG. 15: Time dependence of concentrations of atomic deuterium (open triangles) and atomic hydrogen (open circles) in different Im-He solids stored at $T = 1.35$ K.

with recombinational decay in the sample produced from a $H_2:D_2:He=1:4:100$ mixture. In Fig.15c the population of hydrogen atoms actually shows an increase which is driven by the chemical reactions as time evolves. The large initial supply of deuterium molecules in the gas mixture $H_2:D_2:He = 1:8:180$ means that a copious supply of deuterium atoms is available in the sample, leading to a higher production of hydrogen atoms.

The chemical reactions discussed above were hypothesized by Gordon *et al.* [9] for impurity-helium solids to explain the unexpectedly high initial populations of hydrogen atoms when impurity-helium solids containing hydrogen and deuterium atoms were formed in their experiments. They were not able to determine the time evolution of the concentrations of the two species in their experiments, however. Later these chemical reactions have been employed to study chemical reactions in solid hydrogen matrices by Ivliev *et al.* [23] via deposition of the products of H_2 and D_2 passing through a radio frequency discharge and Miyazaki *et al.* [24–28] in experiments on γ -irradiated samples of solid mixtures of H_2 and D_2 . Both of these groups monitored the populations of atomic hydrogen and deuterium as a function of time following the deposition or irradiation. Although the concentrations of

hydrogen and deuterium atoms were very dilute in their work, time evolutions were found to be similar to the results of our experiments.

Since all of the experiments involving these chemical reactions are performed at liquid helium temperatures, thermally activated processes can be effectively ruled out. When a deuterium atom is adjacent to a molecule of hydrogen, an intermediate state involving the metastable compound molecule HDH is formed. Then a hydrogen atom is emitted, leaving behind a stable HD molecule. The potential barrier for the formation of the compound molecule is typically of order 4000 K [29] which is far greater than liquid helium temperatures (1-4 K), justifying our statement that the reactions are not thermally activated. Therefore the reactions can be driven only by quantum mechanical tunneling and are thus classified as exchange tunneling reactions.

In studying the sample evolution, we must take into account the reaction rates for the two chemical reactions we have discussed. According to the theoretical work of Takayanagi *et al.* [30], the rate for the reaction $D+H_2\rightarrow HD+H$ is two orders of magnitude faster than for $D+HD\rightarrow D_2+H$. The unexpectedly high initial concentrations of hydrogen atoms seen in our work and that of Gordon *et al.* [9] are attributable to the very high rate for the former reaction, where we estimate the time constant to be on the order of one minute for our samples. The slower decay after sample formation is in large part attributable to the latter reaction. Assuming that the process $D+HD\rightarrow D_2+H$ is the leading mechanism of depletion of the deuterium atom concentration $[D]$ in the sample prepared from $H_2:D_2:He=1:4:100$ mixture, we calculate the rate constant k for this reaction:

$$\frac{d[D]}{dt} = -k [HD] [D] \quad (2)$$

For this sample the measured decay time of $[D]$ is $\tau_D = (d[D]/dt/[D])^{-1} \simeq 550$ min (Fig.15b). To calculate the concentration of HD molecules $[HD]$ we shall assume complete dissociation of H_2 and D_2 molecules passing through the RF discharge during sample preparation. Recombination reactions will take place in the warm beam as it travels toward the superfluid surface with the resulting formation of H_2 , HD and D_2 molecules, which are in turn incorporated into the impurity-helium solids with the initial molecular ratio $H_2:HD:D_2 = 1:8:16$ [31]. Deuterium atoms react rapidly with the H_2 molecules in the sample, resulting in the formation of additional HD molecules. Therefore after a few minutes the ratio of HD: D_2 will become closer to 9:16. Assuming the cluster density to be close to that of solid deuterium

[12], we find an HD concentration of approximately $1.7 \cdot 10^{22} \text{ cm}^{-3}$. Then $k \simeq 1.1 \cdot 10^{-3} \text{ cm}^3 \text{ mol}^{-1} \text{ s}^{-1}$, which is consistent with Miyazaki's value of k for D in a solid HD sample. This agreement provides further evidence that small clusters of impurities are very important in determining the properties of impurity-helium solids.

In conclusion, we point out that matrix isolation of reactive atomic species in impurity-helium solids greatly impedes molecular recombination reactions. The results of our work indicate that the atoms tend to be associated with clusters of other impurity atoms and molecules. They do not appear to simply occur as individual atoms isolated by layers of solid helium. Two pieces of evidence support this conclusion. One of these is that the satellite lines in our ESR spectra indicate that neighboring H_2 and HD molecules are close to the hydrogen and deuterium atoms. The second is that the rate constants seen in the exchange tunneling reactions are consistent with clustering.

The exchange tunneling reactions are capable of producing very high concentrations of hydrogen atoms. Our best estimates from the ESR line intensity measurements indicate average concentrations $\sim 10^{18} \text{ atoms/cm}^3$. For this concentration the thermal de Broglie wave length becomes comparable to the mean distance between hydrogen atoms at $\sim 30 \text{ mK}$ which can possibly be reached by means of a dilution refrigerator, provided that recombinational heat and the heat from ortho-para conversion of hydrogen molecules can be removed efficiently. Quantum overlap phenomena involving quantum statistical effects or magnetic transitions might be observable. The local concentration of hydrogen atoms within a cluster is much larger than the average concentration, so that quantum overlap of the hydrogen atoms may occur at much higher temperatures. If the clusters containing hydrogen atoms are above the percolation threshold, we indulge in the speculation that dramatic transport properties associated with Bose-Einstein condensation (BEC) might be observable. Relevant to this discussion, Toennies and co-workers [32] have recently observed a phenomenon that they have interpreted as superfluidity of H_2 trapped in isolated clusters. Reppy and co-workers [33] have performed seminal studies of BEC in a very dilute film of liquid helium trapped in the pores of Vycor glass in the 1980's, anticipating later studies of BEC in the alkali gases and spin polarized hydrogen gas.

Finally, the forbidden line has been observed for the first time in hydrogen atoms trapped in an impurity helium solid. This sets the stage for possible dynamic nuclear polarization experiments.

ACKNOWLEDGEMENTS

The authors wish to thank NASA for supporting this work via NASA grant NAG 8-1445.

- [1] A.M. Bass and H.P. Broida, "Formation and Trapping of Free Radicals" (Academic Press, New York 1960)
- [2] J.L. Jackson, *Formation and Trapping of Free Radicals*, edited by A.M. Bass and H.P. Broida (Academic Press, New York and London, 1960), p. 327
- [3] E.B. Gordon, L.P. Mezhov-Deglin, O.F. Pugachev, *JETP Lett.* **19**, 63 (1974).
- [4] E.B. Gordon, V.V. Khmelenko, E.A. Popov, A.A. Pelmenev, O.F. Pugachev, *Chem. Phys. Lett.* **155**, 301 (1989)
- [5] E.B. Gordon, V.V. Khmelenko, A.A. Pelmenev, E.A. Popov, O.F. Pugachev, A.F. Shestakov, *Chem. Phys.* **170**, 411 (1993)
- [6] R.E. Boltnev, E.B. Gordon, V.V. Khmelenko, I.N. Krushinskaya, M.V. Martynenko, A.A. Pelmenev, E.A. Popov, A.F. Shestakov, *Chem. Phys.* **189**, 367 (1994)
- [7] R.E. Boltnev, E.B. Gordon, V.V. Khmelenko, M.V. Martynenko, A.A. Pelmenev, E.A. Popov, A.F. Shestakov, *J. de Chimie Physique* **92**, 362 (1995)
- [8] R.E. Boltnev, I.N. Krushinskaya, A.A. Pelmenev, D.Yu. Stolyarov, V.V. Khmelenko, *Chem. Phys. Lett.* **305**, 217 (1999)
- [9] E.B. Gordon, A.A. Pelmenev, O.F. Pugachev, and V.V. Khmelenko, *JETP Lett.* **37**, 282 (1983)
- [10] E.B. Gordon, A.A. Pelmenev, O.F. Pugachev, V.V. Khmelenko *Sov. J. Low Temp. Phys.* **11**, 307 (1985)
- [11] B. R. Jonson *et. al*, *Phys. Rev. Lett.* **52**, 1508 (1984); N. P. Bigelow, J. H. Freed, D. M. Lee, *Phys. Rev. Lett.* **63**, 1609 (1989)
- [12] S.I. Kiselev *et. al*, *Phys. Rev. B* **65**, 024517 (2002)
- [13] S.I. Kiselev, V.V. Khmelenko, D.A. Geller, J.R. Beamish, and D.M. Lee, *J. Low Temp. Phys.* **119**, 357 (2000)
- [14] S.I. Kiselev, V.V. Khmelenko, and D.M. Lee, *Low Temp. Phys.* **26**, 641 (2000)
- [15] V. Kiryukhin, B Keimer, R.E. Boltnev, V.V. Khmelenko, E.B. Gordon, *Phys. Rev. Lett.* **79**,

1774 (1997)

- [16] S.I. Kiselev *et al.* *J. Low Temp. Phys.* **126**, 235 (2002)
- [17] S.I. Kiselev *et al.* *J. Low Temp. Phys.* **128**, 37 (2002)
- [18] N.F. Ramsey, *Molecular Beams* (Clarendon Press, Oxford, 1956, London-Sydney, 1963)
- [19] A. Abragam and M. Goldman, *Nuclear Magnetism: Order and Disorder* (Clarendon Press, Oxford, 1982)
- [20] T. Miyazaki *et al.* *J. Phys. Chem* **94**, 1702 (1990)
- [21] G.T. Trammell *et al.* *Phys. Rev.* **110**, 630 (1958)
- [22] Yu. Kagan *et al.* *JETP Lett.* **36**, 253 (1982)
- [23] A.V. Ivliev *et al.*, *JETP Lett.* **38**, 379 (1983)
- [24] H. Tsuruta, T. Miyazaki, K. Fueki, N. Azuma, *J. Phys. Chem.* **87**, 5422 (1983);
- [25] T. Miyazaki, K.-P. Lee, K. Fueki, and A. Takeuchi, *J. Phys. Chem.* **88**, 4959 (1984),
- [26] T. Miyazaki, N. Iwata, K.-P. Lee, K. Fueki, *J. Phys. Chem.* **93**, 3352 (1989),
- [27] T. Kumada *et al.* *Chem. Phys. Lett.* **261**, 463 (1996)
- [28] T. Kumada *et al.* *J. Chem. Phys.* **116**, 1109 (2002)
- [29] R.N. Porter and M. Karplus, *J. Chem. Phys.* **40**, 1105 (1964)
- [30] T. Takayanagi *et al.* *J. Chem. Phys.* **90**, 1641 (1989)
- [31] S.I. Kiselev, Ph.D. thesis, Cornell University, 2002 (unpublished)
- [32] J.P. Toennies *et al.* *Phys. Today* **54(2)**, 31 (2001)
- [33] B.C. Crooker *et al.* *Phys. Rev. Lett.* **51**, 666 (1983)

LIST OF PUBLICATIONS FOR NASA GRANT NAG 8-1445

1. S.I. Kiselev, V.V. Khmelenko, D.A. Geller, J.R. Beamish, and D.M. Lee, "Investigation of ultrasound propagation in impurity-helium solids", *Physica B* **284-288**, 105-106 (2000)
2. S.I. Kiselev, V.V. Khmelenko, D.A. Geller, J.R. Beamish, and D.M. Lee, "Investigation of Ultrasound Propagation in Porous Impurity-Helium Solids", *J. Low Temp. Phys.* **119**, 357-366 (2000)
3. S.I. Kiselev, V.V. Khmelenko, and D.M. Lee, "Sound propagation in liquid He in impurity-helium solids", *Low Temp. Phys.* **26**, 641-648 (2000)
4. S.I. Kiselev, V.V. Khmelenko, and D.M. Lee, "Investigation of Ultrasound Attenuation in Impurity-Helium Solids Containing Liquid Helium", *J. Low Temp. Phys.* **121**, 671-676 (2000)
5. S.I. Kiselev, V.V. Khmelenko, C.Y. Lee and D.M. Lee, "Hyperfine Resonance of Deuterium Atoms Stabilized in Impurity-Helium Solids", *J. Low Temp. Phys.* **121**, 677-682 (2000)
6. S.I. Kiselev, V.V. Khmelenko, D. M. Lee, V. Kiryukhin, R.E. Boltnev, E.B. Gordon, and B. Keimer, "Structural studies of impurity-helium solids", *Phys. Rev. B* **65**, 024517 (2002)
7. S.I. Kiselev, V.V. Khmelenko, D. M. Lee, V. Kiryukhin, R.E. Boltnev, E.B. Gordon, and B. Keimer, "X-ray Studies of Structural Changes of Impurity- Helium Solids", *J. Low Temp. Phys.* **126**, 235-240 (2002)
8. S.I. Kiselev, V.V. Khmelenko, D. M. Lee and C.Y. Lee, "Magnetic Resonance Studies of Impurity-Helium Solids Containing Hydrogen and Deuterium Impurities", *J. Low Temp. Phys.* **128**, 37-52 (2002)
9. V.V. Khmelenko, S.I. Kiselev, D. M. Lee and C.Y. Lee, "Impurity -Helium Solids - Quantum Gels?", *Physica Scripta*, **T102**, 118-127 (2002)
10. S.I. Kiselev, V.V. Khmelenko, D. M. Lee, " Hydrogen Atoms in Impurity -Helium Solids", *Phys. Rev. Lett.*, **89**, 175301 (2002)
11. S.I. Kiselev, "Impurity - Helium Solids", PhD thesis, Cornell University, 2002

REPORT DOCUMENTATION PAGE

Form Approved
OMB No. 0704-0188

Public reporting burden for this collection of information is estimated to average 1 hour per response, including the time for reviewing instructions, searching data sources, gathering and maintaining the data needed, and completing and reviewing the collection of information. Send comments regarding this burden estimate or any other aspect of this collection of information, including suggestions for reducing this burden to Washington Headquarters Service, Directorate for Information Operations and Reports, 1215 Jefferson Davis Highway, Suite 1204, Arlington, VA 22202-4302, and to the Office of Management and Budget, Paperwork Reduction Project (0704-0188) Washington, DC 20503.

PLEASE DO NOT RETURN YOUR FORM TO THE ABOVE ADDRESS.

1. REPORT DATE (DD-MM-YYYY)		2. REPORT DATE April 30, 2003		3. DATES COVERED (From - To) 02/01/98 - 01/31/03		
4. TITLE AND SUBTITLE Studies of Atomic Free Radicals Stored in a Cryogenic Environment				5a. CONTRACT NUMBER		
				5b. GRANT NUMBER NASA NAG8-1445		
				5c. PROGRAM ELEMENT NUMBER		
6. AUTHOR(S) David M. Lee, Principal Investigator				5d. PROJECT NUMBER		
				5e. TASK NUMBER		
				5f. WORK UNIT NUMBER		
7. PERFORMING ORGANIZATION NAME(S) AND ADDRESS(ES) Lab of Atomic and Solid State Physics Clark Hall 117, Cornell University Ithaca, NY 14853				8. PERFORMING ORGANIZATION REPORT NUMBER		
9. SPONSORING/MONITORING AGENCY NAME(S) AND ADDRESS(ES) National Aeronautics and Space Administration				10. SPONSOR/MONITOR'S ACRONYM(S) NASA		
				11. SPONSORING/MONITORING AGENCY REPORT NUMBER		
12. DISTRIBUTION AVAILABILITY STATEMENT						
13. SUPPLEMENTARY NOTES Dorothy Hubbard SD-13 & Glen Alexander Marshall Space Flight Center Technical Monitor						
14. ABSTRACT Impurity-Helium Solids are porous gel-like solids consisting of impurity atoms and molecules surrounded by thin layers of solid helium. They provide an ideal medium for matrix isolation of free radicals to prevent recombination and store chemical energy. In this work electron spin resonance, nuclear magnetic resonance, X ray diffraction and ultrasound techniques have all been employed to study the properties of these substances. Detailed studies via electron spin resonance of exchange tunneling chemical reactions involving hydrogen and deuterium molecular and atomic impurities in these solids have been performed and compared with theory. Concentrations of hydrogen approaching the quantum solid criterion have been produced. Structured studies involving X ray diffraction, ultrasound, and electron spin resonance have shown that the impurities in impurity helium solids are predominantly contained in impurity clusters, with each cluster being surrounded by thin layers of solid helium.						
15. SUBJECT TERMS Impurity Helium Solids Matrix isolation of free radicals Quantum Fluids Porous gel-like solids Cryogenic chemical energy storage Clustering Magnetic Resonance Exchange tunneling chemical reactions						
16. SECURITY CLASSIFICATION OF:			17. LIMITATION OF ABSTRACT	18. NUMBER OF PAGES 82	19a. NAME OF RESPONSIBLE PERSON David M. Lee	
a. REPORT	b. ABSTRACT	c. THIS PAGE			19b. TELEPHONE NUMBER (Include area code) 607/255-5286	